

# Single-Walled Carbon Nanotubes Exhibit Strong Antimicrobial Activity

Seoktae Kang, Mathieu Pinault,<sup>†</sup> Lisa D. Pfefferle, and Menachem Elimelech\*

Department of Chemical Engineering, Yale University, P.O. Box 208286,  
New Haven, Connecticut 06520-8286

Received April 12, 2007. In Final Form: June 12, 2007

We provide the first direct evidence that highly purified single-walled carbon nanotubes (SWNTs) exhibit strong antimicrobial activity. By using a pristine SWNT with a narrow diameter distribution, we demonstrate that cell membrane damage resulting from direct contact with SWNT aggregates is the likely mechanism leading to bacterial cell death. This finding may be useful in the application of SWNTs as building blocks for antimicrobial materials.

Carbon-based nanomaterials, such as fullerene and carbon nanotubes (CNTs), exhibit unique size- and structure-dependent optical, electronic, magnetic, thermal, chemical, and mechanical properties.<sup>1</sup> As a result, it is not surprising that these nanomaterials have been considered for use in numerous applications, including the fabrication of superconductors, optical devices, sensors, energy storage devices, fuel cells, and catalysts.<sup>2</sup> However, such extraordinary physical and chemical properties are accompanied by concerns about possible adverse effects of these materials on biological systems. In particular, applications that use single-walled carbon nanotubes (SWNTs) for biosensors,<sup>3</sup> drug and vaccine delivery transporters,<sup>4,5</sup> and novel biomaterials<sup>6</sup> increase the potential for encounters between SWNTs and humans and the ecosystem. Future commercial development of nanotechnology may also lead to the discharge of SWNTs into the environment.

Information concerning the potential toxicity from exposure to SWNTs and their environmental impact is scarce, often debated,<sup>7</sup> and focused on human cells.<sup>8–11</sup> The toxicity of SWNTs to human cells has been observed to vary with SWNT functionalization and the concentration of the solubilizing agent (i.e., surfactants),<sup>12,13</sup> as well as with SWNT physicochemical properties such as structure, diameter, cleanliness (e.g., % metal),

\* Corresponding author. E-mail: menachem.elimelech@yale.edu.  
Phone: +1 (203) 432-2789. Fax: +1 (203) 432-2881.

<sup>†</sup> Current address: Laboratoire Francis Perrin, 91191 Gif sur Yvette Cedex, France.

(1) Salvétat, J. P.; Briggs, G. A. D.; Bonard, J. M.; Bacsa, R. R.; Kulik, A. J.; Stockli, T.; Burnham, N. A.; Forro, L. *Phys. Rev. Lett.* **1999**, *82*, 944–947.

(2) Balasubramanian, K.; Burghard, M. *Small* **2005**, *1*, 180–192.

(3) Chen, R. J.; Bangsaruntip, S.; Drouvalakis, K. A.; Kam, N. W. S.; Shim, M.; Li, Y. M.; Kim, W.; Utz, P. J.; Dai, H. J. *Proc. Natl. Acad. Sci. U.S.A.* **2003**, *100*, 4984–4989.

(4) Kam, N. W. S.; O'Connell, M.; Wisdom, J. A.; Dai, H. J. *Proc. Natl. Acad. Sci. U.S.A.* **2005**, *102*, 11600–11605.

(5) Liu, Z.; Cai, W.; He, L.; Nakayama, N.; Chen, K.; Sun, X.; Chen, X.; Dai, H. *Nat. Nanotechnol.* **2007**, *2*, 47–51.

(6) Narayan, R. J.; Berry, C. J.; Brignon, R. L. *Mater. Sci. Eng., B* **2005**, *123*, 123–129.

(7) Worle-Knirsch, J. M.; Pulskamp, K.; Krug, H. F. *Nano Lett.* **2006**, *6*, 1261–1268.

(8) Ding, L. H.; Stilwell, J.; Zhang, T. T.; Elboudwarej, O.; Jiang, H. J.; Selegue, J. P.; Cooke, P. A.; Gray, J. W.; Chen, F. Q. *Nano Lett.* **2005**, *5*, 2448–2464.

(9) Manna, S. K.; Sarkar, S.; Barr, J.; Wise, K.; Barrera, E. V.; Jejelowo, O.; Rice-Ficht, A. C.; Ramesh, G. T. *Nano Lett.* **2005**, *5*, 1676–1684.

(10) Jia, G.; Wang, H. F.; Yan, L.; Wang, X.; Pei, R. J.; Yan, T.; Zhao, Y. L.; Guo, X. B. *Environ. Sci. Technol.* **2005**, *39*, 1378–1383.

(11) Magrez, A.; Kasas, S.; Salicio, V.; Pasquier, N.; Seo, J. W.; Celio, M.; Caticas, S.; Schwaller, B.; Forro, L. *Nano Lett.* **2006**, *6*, 1121–1125.

(12) Sayes, C. M.; Liang, F.; Hudson, J. L.; Mendez, J.; Guo, W. H.; Beach, J. M.; Moore, V. C.; Doyle, C. D.; West, J. L.; Billups, W. E.; Ausman, K. D.; Colvin, V. L. *Toxicol. Lett.* **2006**, *161*, 135–142.

(13) Chen, X.; Tam, U. C.; Czlapinski, J. L.; Lee, G. S.; Rabuka, D.; Zettl, A.; Bertozzi, C. R. *J. Am. Chem. Soc.* **2006**, *128*, 6292–6293.

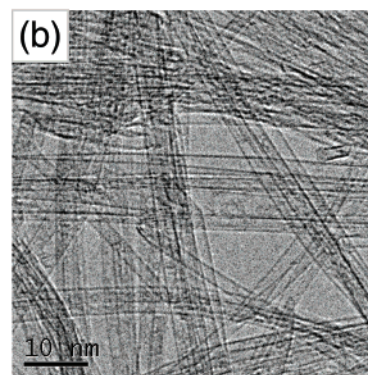
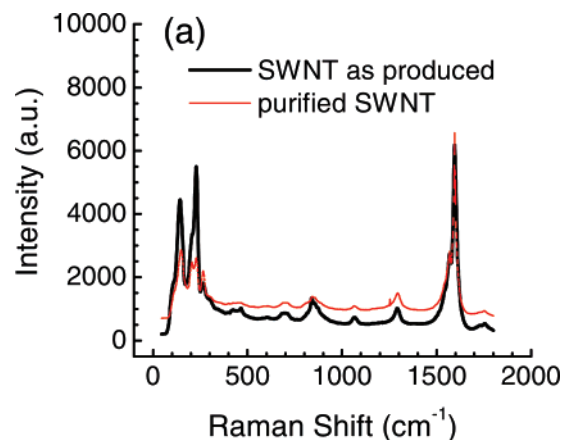


**Figure 1.** Characterization of SWNTs. (a) Raman spectroscopy (785 nm) of SWNTs before and after purification. (b) TEM image of purified SWNTs.

and defect level.<sup>14</sup> In these studies, however, commercial SWNTs were used, and characterization was not well defined. Furthermore, for these SWNTs, factors such as mean diameter, diameter distribution, metal content, and defect level cannot be independently varied because of limitations of the SWNT synthesis, cleaning, and separation processes. Commercial SWNTs have generally been treated with strong acids and contain on average 4.5–15% metal and other impurities.<sup>15</sup> Only a handful of groups can produce SWNTs with a narrow diameter distribution.<sup>16</sup>

The above studies with human cells may suggest that SWNTs can also interact with microbes and exhibit antimicrobial

(14) Karakoti, A. S.; Hench, L. L.; Seal, S. *JOM* **2006**, *58*, 77–82.

(15) Zhao, B.; Itkis, M. E.; Niyogi, S.; Hu, H.; Zhang, J.; Haddon, R. C. *J. Phys. Chem. B* **2004**, *108*, 8136–8141.

(16) Chen, Y.; Ciuparu, D.; Lim, S.; Yang, Y. H.; Haller, G. L.; Pfefferle, L. *J. Catal.* **2004**, *226*, 351–362.

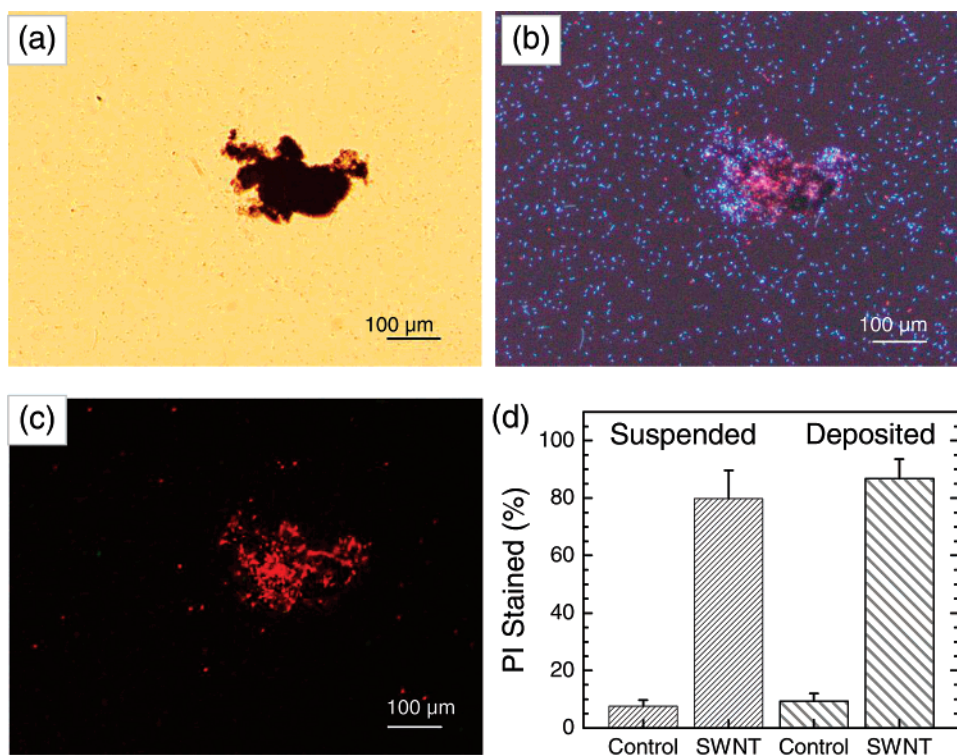


**Figure 2.** Cell viability measurements after exposure to SWNTs ( $5 \mu\text{g/mL}$ ) in an isotonic solution ( $0.9\%$  NaCl,  $\text{pH } 5.6 \pm 0.1$ ). (a) Microscopic image of SWNT aggregates. (b) Fluorescence microscope image of total cells (cells stained with propidium iodide and DAPI). (c) Fluorescence microscope image of dead cells (stained with propidium iodide only). (d) Fluorescence-based assay showing the antimicrobial activity of SWNTs as the percent of cells stained with PI or the percent of loss of viability (with error bars representing 1 SD). Data are shown for suspended SWNT aggregates and for SWNTs deposited layer.

properties. Surprisingly, however, no published studies exist on the direct interaction of SWNTs with microbes. In this work, we investigate the interaction of well-characterized, low metal content, narrowly distributed, pristine SWNTs with model bacteria *Escherichia coli* K12. Our experiments provide the first direct evidence that highly purified SWNTs exhibit strong antimicrobial activity and indicate that severe cell membrane damage by direct contact with SWNTs is the likely mechanism responsible for the toxicity to the model bacteria. These observations point to the potential use of SWNTs as building blocks for antimicrobial materials.

To assess the biotoxicity of SWNTs on *E. coli* K12, we first prepared SWNTs, which had more than 90% selectivity to raw SWNTs, by CO disproportionation over highly dispersed cobalt-substituted MCM-41 and an amorphous silica catalyst.<sup>17</sup> Consequently, purification was very mild. Multiwavelength excitation Raman spectra demonstrated that the whole purification procedure did not produce many defects in the SWNTs (the G/D band ratio is essentially unchanged) and that the SWNT structure is well preserved (as evidenced by the Raman breathing mode) (Figure 1a). TEM analysis of the SWNTs shows that the tube diameters ranged from 0.75 to 1.2 nm, with a mean diameter of around 0.9 nm. Using mild acid cleaning, we achieved nearly complete removal of cobalt (less than 0.8 wt % based on elemental analysis) and amorphous carbon (by thermogravimetric analysis, data not shown) for the SWNTs used. SWNTs prepared in this manner are not highly bundled as shown in Figure 1b.

We then tested the viability of *E. coli* K12 following their interaction with SWNTs in aqueous solution. Large SWNT aggregates were formed during the incubation period (Figure 2a). The favorable attachment and almost complete coverage of

*E. coli* on the exposed surface of the SWNT aggregates (Figure 2b) rendered cell counting techniques, such as the use of a cell-counting chamber and flow cytometry, impractical. Hence, we applied an area-based determination of microbial viability (details in Supporting Information) for these experiments involving the interaction of *E. coli* cells with suspended SWNTs in the saline solution.

Because SWNTs are capable of interacting with widely used tetrazolium salts (e.g., MTT) and luminescing intrinsically near 520 nm,<sup>7,18</sup> we selected propidium iodide (PI) and 4'-6-diamidino-2-phenylindole (DAPI) to assess the cytotoxicity of SWNTs. These fluorescent dyes did not significantly interact or overlap with the SWNT emission spectra. Our fluorescence-based assays showed that cells incubated with pristine SWNTs for 60 min exhibited a substantial loss in viability (Figure 2c). The percentage of inactivated or compromised *E. coli* cells (i.e., PI-stained) on SWNT aggregates averaged  $79.9 \pm 9.8\%$ , which was significantly higher than the average of the control ( $7.6 \pm 2.1\%$  without SWNT) under similar conditions (Figure 2d). Notably, the free-swimming cells in the sample with SWNTs exhibited no significant difference in viability ( $7.2 \pm 2.4\%$ ) compared to that of the control.

Additional experiments with doses of SWNT ranging from 1 to  $50 \mu\text{g/mL}$  confirmed that the viability of the free-swimming cells was independent of the SWNT dose whereas cells on SWNT aggregates always exhibited a substantial loss of viability. The above results imply that direct contact between cells and SWNT aggregates was essential for the inactivation of *E. coli* cells. We also found that the biotoxicity was dependent on the bacterial incubation time with SWNTs. The average percentages of loss of viability (i.e., PI-stained) for cells on SWNT aggregates were  $73.1 \pm 5.4\%$ ,  $79.9 \pm 9.8\%$ , and  $87.6 \pm 4.7\%$  for 30, 60, and 120

(17) Lim, S.; Ciuparu, D.; Pak, C.; Dobek, F.; Chen, Y.; Harding, D.; Pfefferle, L.; Haller, G. *J. Phys. Chem. B* **2003**, *107*, 11048–11056.

(18) Guldi, D. M.; Holzinger, M.; Hirsch, A.; Georgakilas, V.; Prato, M. *Chem. Commun.* **2003**, 1130–1131.

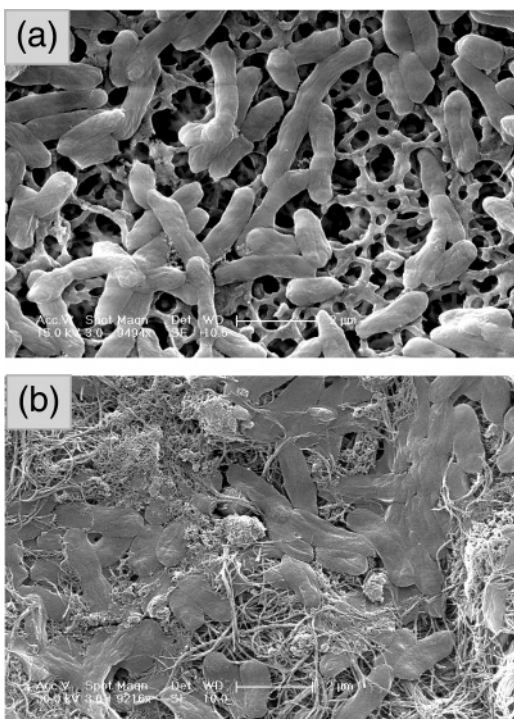


**Figure 3.** Scanning electron microscopy (SEM) images of *E. coli*. (a) Cells incubated without SWNTs for 60 min. Cells were filtered and observed via SEM on the filter. (b) Cells incubated with SWNTs for 60 min.

min incubation times, respectively. No significant change was observed for the control cells under the same conditions.

To further verify the antimicrobial activity of SWNTs and the validity of the area-based determination of microbial viability, we prepared a SWNT-coated filter (details in Supporting Information). *E. coli* cells were gently filtered so that they would accumulate on the top of the SWNT-coated filter and could be enumerated as individual cells. Results showed that  $86.8 \pm 6.8\%$  of the cells (number-based) on the SWNT-coated filter were stained with PI after the 60 min incubation (Figure 2d). This finding is in agreement with the previously described results of cells interacting with the suspended SWNT aggregates. The results also confirm that direct contact between *E. coli* and SWNTs is necessary for the inactivation of the model bacteria.

To further confirm the antimicrobial activity of SWNTs based on PI staining (indicative of cells with damaged or compromised membranes), we assessed the metabolic activity of cells exposed to SWNTs with 5-cyano-2,3-ditoly-tetrazolium chloride (CTC).<sup>19</sup> We found that only  $6.6 \pm 4.7\%$  of cells were stained with CTC (i.e., metabolically active) whereas the majority of cells ( $74.0 \pm 7.3\%$ ) on the PVDF membrane with no SWNTs (serving as a control) were metabolically active.

We then determined changes in the morphology of *E. coli* cells exposed to SWNTs. The scanning electron microscopy (SEM) images showed that the cells in the control (without SWNTs) were intact and maintained their outer membrane structure (Figure 3a). In contrast, cells that were incubated with SWNTs lost their cellular integrity (Figure 3b). The morphological change of SWNT-treated cells is attributable to cell membrane damage as discussed below.

On the basis of the fluorescence dye tests (Figure 2) and SEM images (Figure 3), we conclude that *E. coli* cells in contact with SWNT aggregates or an SWNT-deposited layer suffered

membrane damage that likely resulted in compromised membrane permeability. The apparent cell damage should have led to an efflux of cytoplasmic materials into the solution. We proved the efflux of cytoplasmic materials by two independent measurements, namely, the concentrations of DNA and RNA in solutions of *E. coli* cells incubated with and without SWNTs. Even without taking into account the adsorption of plasmid DNA and RNA to SWNTs, we measured more than a 5-fold increase of plasmid DNA and a 2-fold increase of RNA in solutions in contact with SWNTs. The significant increase in the concentration of plasmid DNA and RNA in the presence of SWNTs confirms the severe damage to cell membrane integrity.

Although our results show that the *E. coli* undergoes severe membrane damage and subsequent loss of viability due to SWNTs, very little information is currently available with regard to the cytotoxic mechanisms of SWNTs. Previous studies, mainly focusing on mammalian cells, have proposed three principal cytotoxic mechanisms: oxidative stress,<sup>9</sup> metal toxicity,<sup>20</sup> and physical piercing.<sup>6</sup> Of these, our results showed that metal toxicity was not an important mechanism of SWNT toxicity because we were effectively able to purify the SWNTs, resulting in residual metal catalyst (mainly Co) measuring less than 0.8 wt % (which is equivalent to 40 ppb). Several studies have proposed oxidative stress as a direct cause of membrane damage with carbon-based nanomaterials, which is caused by lipid peroxidation within the mammalian cell.<sup>8,9,12</sup> However, these studies centered around the presence of residual metals within CNTs, which may lead to oxidative stress.<sup>21</sup> In fact, recent studies suggest that the physical interaction of carbon-based nanomaterials (fullerene) with cells, rather than oxidative stress, is the primary killing mechanism.<sup>22,23</sup>

Several recent studies suggest that peptide or lipid nanotubes can penetrate through cell membranes because of their cylindrical shape and high aspect ratio and lead to cell death.<sup>24,25</sup> Owing to similarities in geometry, functionalized SWNTs were also able to penetrate cell membranes.<sup>26</sup> Interestingly, results from molecular dynamics simulations can be used to explain the higher antimicrobial activity of smaller-diameter nanotubes such as SWNTs in comparison to that of larger-diameter nanotubes.<sup>10,27</sup> In this study, we postulate that SWNT aggregates caused irrecoverable damage to the *E. coli* bacteria by physical damage to the outer membrane of the cells, causing the release of intracellular content.

In summary, our study provides the first direct confirmation that pristine SWNTs can exhibit strong antimicrobial activity. By using highly purified, pristine SWNTs with a narrow diameter distribution, we demonstrate that direct cell contact with SWNTs can cause severe membrane damage and subsequent cell inactivation. Our finding suggests that SWNTs can be useful as building blocks for antimicrobial materials.

(20) Shvedova, A. A.; Kisin, E. R.; Mercer, R.; Murray, A. R.; Johnson, V. J.; Potapovich, A. I.; Tyurina, Y. Y.; Gorelik, O.; Arepalli, S.; Schwegler-Berry, D.; Hubbs, A. F.; Antonini, J.; Evans, D. E.; Ku, B. K.; Ramsey, D.; Maynard, A.; Kagan, V. E.; Castranova, V.; Baron, P. *Am. J. Physiol.* **2005**, *289*, L698–L708.

(21) Geslin, C.; Llanos, J.; Prieur, D.; Jeanthon, C. *Res. Microbiol.* **2001**, *152*, 901–905.

(22) Ali, S. S.; Hardt, J. I.; Quick, K. L.; Kim-Han, J. S.; Erlanger, B. F.; Huang, T. T.; Epstein, C. J.; Dugan, L. L. *Free Radical Biol. Med.* **2004**, *37*, 1191–1202.

(23) Tang, Y. J.; Ashcroft, J. M.; Chen, D.; Min, G. W.; Kim, C. H.; Murkhejee, B.; Larabell, C.; Keasling, J. D.; Chen, F. Q. *Nano Lett.* **2007**, *7*, 754–760.

(24) Lee, S. B.; Koepsel, R.; Stolz, D. B.; Warriner, H. E.; Russell, A. J. *J. Am. Chem. Soc.* **2004**, *126*, 13400–13405.

(25) Chipot, C.; Tarek, M. *Phys. Biol.* **2006**, *3*, S20–S25.

(26) Kostarelos, K.; Lacerda, L.; Pastorin, G.; Wu, W.; Wieckowski, S.; Luangsilavilay, J.; Godefroy, S.; Pantarotto, D.; Briand, J. P.; Muller, S.; Prato, M.; Bianco, A. *Nat. Nanotechnol.* **2007**, *2*, 108–113.

(27) Lopez, C. F.; Nielsen, S. O.; Moore, P. B.; Klein, M. L. *Proc. Natl. Acad. Sci. U.S.A.* **2004**, *101*, 4431–4434.

(19) Creach, V.; Baudoux, A. C.; Bertru, G.; Le Rouzic, B. *J. Microbiol. Methods* **2003**, *52*, 19–28.

**Acknowledgment.** We acknowledge the support of the National Science Foundation under research grant BES-0646247.

**Supporting Information Available:** Materials and methods. Area-based estimation of viable and dead cells. This material is available free of charge via the Internet at <http://pubs.acs.org>.

**Note Added after ASAP Publication.** This article was published ASAP on July 21, 2007. The caption to Figure 2 has been modified. The correct version was published on July 23, 2007.

LA701067R